Available online at www.sciencedirect.com
ScienceDirect
Journal of Power Sources 162 (2006) 1036–1042
JOURNAL OF POWER SOURCES
www.elsevier.com/locate/jpowsour

Anode-supported solid oxide fuel cell with yttria-stabilized zirconia/gadolinia-doped ceria bilayer electrolyte prepared by wet ceramic co-sintering process

Q.L. Liu *, K.A. Khor, S.H. Chan, X.J. Chen

Fuel Cells Strategic Research Programme, School of Mechanical and Aerospace Engineering, Nanyang Technological University, Singapore 639798, Singapore

Received 22 May 2006; accepted 18 August 2006
Available online 2 October 2006

Abstract

To protect the ceria electrolyte from reduction at the anode side, a thin film of yttria-stabilized zirconia (YSZ) is introduced as an electronic blocking layer to anode-supported gadolinia-doped ceria (GDC) electrolyte solid oxide fuel cells (SOFCs). Thin films of YSZ/GDC bilayer electrolyte are deposited onto anode substrates using a simple and cost-effective wet ceramic co-sintering process. A single cell, consisting of a YSZ (~3 μm)/GDC (~7 μm) bilayer electrolyte, a $La_{0.8}Sr_{0.2}Co_{0.2}Fe_{0.8}O_3$–GDC composite cathode and a Ni–YSZ cermet anode is tested in humidified hydrogen and air. The cell exhibited an open-circuit voltage (OCV) of 1.05 V at 800 °C, compared with 0.59 V for a single cell with a 10-μm GDC film but without a YSZ film. This indicates that the electronic conduction through the GDC electrolyte is successfully blocked by the deposited YSZ film. In spite of the desirable OCVs, the present YSZ/GDC bilayer electrolyte cell achieved a relatively low peak power density of 678 mW cm^{-2} at 800 °C. This is attributed to severe mass transport limitations in the thick and low-porosity anode substrate at high current densities.

Keywords: Solid oxide fuel cell; Yttria-stabilized zirconia film; Gadolinia-doped ceria; Bilayer electrolyte; Anode-supported solid oxide fuel cell; Wet ceramic co-sintering process

1. Introduction

Decrease of the operating temperature of solid oxide fuel cells (SOFCs) from typically ~1000 °C to an intermediate temperature range of 500 to 800 °C, offers many benefits, namely, low material degradation, high system reliability, long stack lifetime, short start-up time, and significant decreases in material requirements and fabrication costs due to the potential utilization of inexpensive and easily machinable metallic materials for the stack. Over the past few years, considerable efforts have been made to lower the operating temperature of SOFCs [1–6]. Three approaches have been adopted: decreasing the electrolyte thickness, utilizing new electrolyte materials with high ionic conductivity at intermediate temperatures, and reducing the electrode polarization resistance. Due to its much higher ionic conductivity at intermediate temperatures than the conventional electrolyte material of yttria-stabilized zirconia (YSZ), doped ceria is regarded as one of the most promising electrolyte candidates for intermediate temperature SOFCs [7].

Many research groups have reported the development of intermediate-temperature SOFCs based on a thin-film electrolyte of doped ceria, which has been fabricated by various processes such as multi-layer tape casting [8], screen printing [9,10], dry pressing [11], spray coating [12,13], and spin coating [3]. Encouraging power densities have been achieved with ceria-based cells at temperatures below 650 °C. Doped ceria is prone, however, to reduction at low oxygen partial pressures [14]. The reduction of ceria from Ce^{4+} to Ce^{3+} will give rise to electronic conduction and thus result in a non-negligible loss in the open-circuit voltage (OCV) of the cell. It will also cause lattice expansion of the ceria electrolyte at the fuel side, and there by lead to mechanical stability problems with the cell or stack [15,16]. To overcome the OCV loss and improve the chemical stability of doped ceria electrolytes in reducing atmo-

* Corresponding author. Tel.: +65 6790 5571; fax: +65 6792 4062.
E-mail address: qlliu@ntu.edu.sg (Q.L. Liu).

0378-7753/$ – see front matter © 2006 Elsevier B.V. All rights reserved.
doi:10.1016/j.jpowsour.2006.08.024

Table 1
Open-circuit voltages of SOFCs with YSZ/doped ceria bilayer electrolytes obtained in this study and from references

Electrolyte composition	Thickness ratio	OCV (V)			Film deposition method	Cell configuration	Reference
		600 °C	700 °C	800 °C			
YSZ/GDC	3 μm/7 μm	1.107	1.081	1.049	Wet ceramic co-sintering process	H_2, Ni–YSZ||YSZ/GDC|| LSCF-GDC, air	This study
YSZ/YDC	1 μm/1.5 mm	0.95	0.89	–	RF sputtering	H_2, Pt ||YSZ/YDC||Pt, O_2	[20]
YSZ/SDC	1.86 μm/1.825 mm	–	–	1.08	RF ion plating	H_2, Pt ||YSZ/SDC||Pt, O_2	[22]
YSZ/SDC	2 μm/0.658 mm	–	–	1.05	RF ion plating	H_2, Ni-YSZ||YSZ/SDC||LSM, O_2	[23]
YSZ/GDC	2 μm/1 mm	0.88	0.80	0.75	RF sputtering	O_2, Pt ||YSZ/GDC||Pt, H_2	[21]
YSZ/YDC	3–3.5 μm/1 mm	0.93	0.88	0.84	EVD + RF sputtering	O_2, Pt ||YSZ/YDC||Pt, H_2	[21]
YSZ/YDC	1.2–2 μm/–	–	0.85	0.79	MOCVD	O_2, Pt ||YSZ/YDC||Pt, H_2	[24]
YSZ/YDC	1 μm/8 μm	1.007	–	–	Reactive sputtering	H_2 + Ar, Ni-YSZ||YSZ/YDC|| LSM-YSZ, air	[25]
YSZ/YDC	0.3 μm/–	0.85	0.79	0.73	Sol–gel spin coating	H_2, Pt ||YSZ/YDC||Pt, O_2	[26]
YSZ/YDC	2 μm/1.6 mm	–	0.92	0.85	Sol–gel spin coating	H_2, Pt ||YSZ/YDC||Pt, O_2	[27]
YSZ/GDC	2 μm/0.44 mm	0.725 (900 °C)			Sol–gel dip coating	H_2, Pt ||YSZ/GDC||Pt, O_2	[28]

spheres, one of the approaches proposed is to coat doped ceria with a very thin YSZ film to form a bilayer electrolyte. In this electrolyte, the YSZ film functions as an electronic blocking layer since YSZ is quite stable under reducing atmosphere conditions.

Since the ionic conductivity of YSZ is very low at intermediate temperatures, the YSZ film as an electronic blocking layer should be sufficiently thin so as to minimize its contribution to the overall resistance of the bilayer electrolyte. From a thermodynamic viewpoint, when the oxygen partial pressure across the ceria electrolyte is higher than the equilibrium value of the Ce_2O_3/CeO_2 redox reaction at a certain temperature, the ceria electrolyte should be chemically stable. Hence, the stability of the bilayer electrolyte will be determined by the interfacial oxygen partial pressure between the YSZ film and the ceria substrate. Theoretical investigations have demonstrated [17–19] that the interfacial oxygen partial pressure is determined by the thickness ratio of the two electrolyte layers and that, generally, a YSZ film of a few μm in thickness should be sufficient to prevent the ceria electrolyte from reduction and thus overcome the OCV loss due to ceria reduction [17–19]. Towards this end, many techniques such as RF sputtering [20,21], ion plating [22,23], electrochemical vapour deposition (EVD) [21], metal–organic chemical vapour deposition (MOCVD) [24], DC sputtering [25] and sol–gel coating [26–28] have been employed to deposit a thin film of YSZ on doped-ceria electrolyte.

By reviewing experimental studies of the YSZ/doped-ceria bilayer electrolyte reported in the literature (see Table 1), four aspects can be summarized. First, except for the work reported by Tsai et al. [25], all the investigations were associated with a thin film of YSZ deposited on a relatively thick substrate of doped ceria (0.4–2 mm). Second, bilayer electrolytes exhibited an improvement in OCV compared with uncoated doped-ceria electrolyte, which demonstrates that YSZ deposition is practically effective in suppressing electronic conduction in the ceria electrolyte. Nevertheless, the improved OCVs are not exceptional as they still exhibit an obvious deviation from the theoretical electromotive forces (EMF), except for the bilayer electrolytes with a YSZ film deposited by ion plating [22,23] or DC sputtering [25]. Third, the fact that the bilayer electrolyte with a 1.86 μm YSZ film deposited by the ion plating on a 1.825 mm samaria-doped ceria (SDC) substrate demonstrated an OCV of 1.08 V at 800 °C in H_2/O_2 atmospheres, which is quite close to the theoretical EMF, does indicate that the OCV loss for doped-ceria electrolyte cells can be satisfactorily avoided by introducing a YSZ thin film with good quality. Fourth, all the above methods used for YSZ film deposition involve either costly equipment (such as ion plating and RF sputtering) or complicated processes (such as sol–gel coating).

In view of these aspects, a wet ceramic process combined with co-sintering was selected to fabricate the thin film of YSZ/GDC bilayer electrolyte in this study because it is a very simple method and does not require any expensive equipment. With this powder-based wet ceramic process, 10-μm bilayer electrolyte thin films consisting of a 3 μm YSZ layer and a 7 μm GDC layer have been successfully obtained after co-sintering with the anode substrate at 1400 °C. Based on a high-quality thin film of YSZ/GDC bilayer electrolyte supported on Ni–YSZ cermet anode substrate, single cells have been assembled with a $L_{0.8}Sr_{0.2}Co_{0.2}Fe_{0.8}O_3$–GDC (50:50 by weight) composite as the cathode and tested in humidified H_2/air atmospheres.

2. Experimental

2.1. Cell fabrication

Commercial powders of 8 mol% Y_2O_3/ZrO_2 (YSZ, Tosoh, Japan) and NiO (J.T. Baker, USA) were used to prepare Ni–YSZ cermet anode supporting substrates. The powders were mixed in a composition of 40 wt.% YSZ and 60 wt.% NiO by ball milling in isopropanol, then the mixture was dried on a hot plate and milled manually using a mortar and a pestle to produce a homogeneously mixed anode powder. The resultant anode powder was compacted into discs under uniaxial pressure using a steel die of 24 mm in diameter. The green anode discs were subsequently pre-fired at 900 °C for 1 h to increase the mechanical strength to facilitate subsequent electrolyte film deposition.

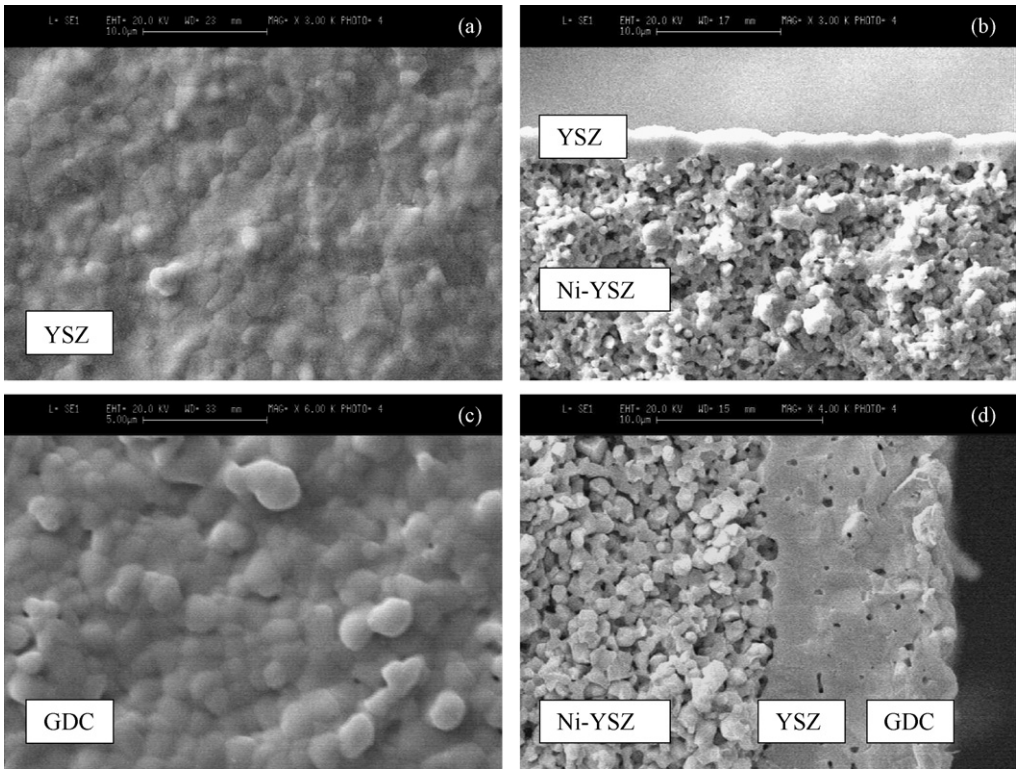

Fig. 1. Scanning electron micrographs of (a) top surface and (b) cross-section of a YSZ film on a reduced anode substrate, and (c) top surface and (d) cross-section of a YSZ/GDC bilayer electrolyte film on a reduced anode substrate.

To prepare anode-supported YSZ/GDC bilayer electrolyte films, suspensions of YSZ and GDC ($Gd_{0.1}Ce_{0.9}O_{1.95}$, Nextech, USA) were applied in sequence to one side of the pre-fired anode discs using a spray-coating method. With the YSZ layer next to the anode, the GDC layer will be protected from the reducing atmosphere, and thus will eliminate electronic conduction through the GDC electrolyte. The suspension of YSZ or GDC was prepared by ultrasonically dispersing a given amount of corresponding powder in isopropanol together with some other organics such as polyethylene glycol 6000 (PG 6000) and polyvinyl butyral (PVB), followed by ball milling for 24 h. The thickness of the deposited YSZ or GDC films was controlled by the powder content in the suspension and spraying times. The coated anode discs were then co-sintered at 1400 °C for 2 h to obtain dense YSZ/GDC bilayer electrolyte films supported on Ni–YSZ cermet anode substrates. After co-sintering, the coated anode substrates were flat and had a diameter of about 18.8 mm and a thickness of about 0.8 mm.

The cathode material consisted of LSCF ($La_{0.8}Sr_{0.2}Co_{0.2}Fe_{0.8}O_3$, Thin Film Components, USA) and GDC (50:50 by weight) and was prepared in the same way as the NiO–YSZ anode powder. The resulting LSCF-GDC composite powder was then mixed with an appropriate amount of polyethylene glycol 400 to form a cathode paste. The paste was applied on the electrolyte side of the coated anode substrates using a screen-printing method and subsequently fired at 900 °C for 2 h. The active area of the cathode was 0.5 cm^2. To ensure a good current collection, a layer of Pt paste was painted on the surface of the LSCF-GDC cathode followed by firing at 900 °C for 30 min.

2.2. Cell tests

The performance characteristics of the prepared anode-supported single cells with YSZ/GDC bilayer electrolytes were evaluated by means of an in-house built SOFC test station. The anode side of the single cell was sealed with a ceramic paste, while the cathode side was not sealed. Platinum gauze with a similar diameter to the cathode (8 mm) was used as the current collector for both the anode and the cathode. Two platinum leads were connected to each platinum gauze to serve as voltage and current probes. During the course of a test, humidified H_2 (3 vol.% H_2O) was fed to the anode and air to the cathode. The NiO in the anode was reduced to Ni *in situ* in the hydrogen atmosphere. The supply of hydrogen and air was controlled by respective mass and rotameter flowmeters. To examine the effect of hydrogen diffusion in the anode substrate on the polarization behaviour of the cell, a gas mixture of hydrogen and nitrogen was also used. Electrochemical measurements were performed with an Autolab PG30/FRA system (Eco Chimie, Netherlands). The OCV data were recorded in the temperature range of 500 to 800 °C. The current–voltage characteristics of the cell were determined from 700 to 800 °C by linear sweep voltammetry at a scan rate of 1 mV s^{-1}.

2.3. Microstructural observations and density measurements

The microstructure of the samples was examined by means of a scanning electron microscope (SEM, Leica 360). The thick-

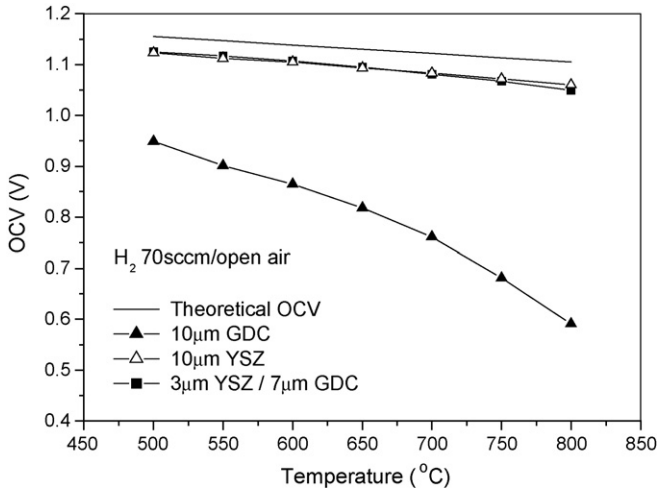

Fig. 2. Theoretical and measured OCV vs. temperature for single cells with 10-μm GDC monolayer electrolyte, 10-μm YSZ monolayer electrolyte, and 3-μm YSZ/7-μm GDC bilayer electrolyte, respectively.

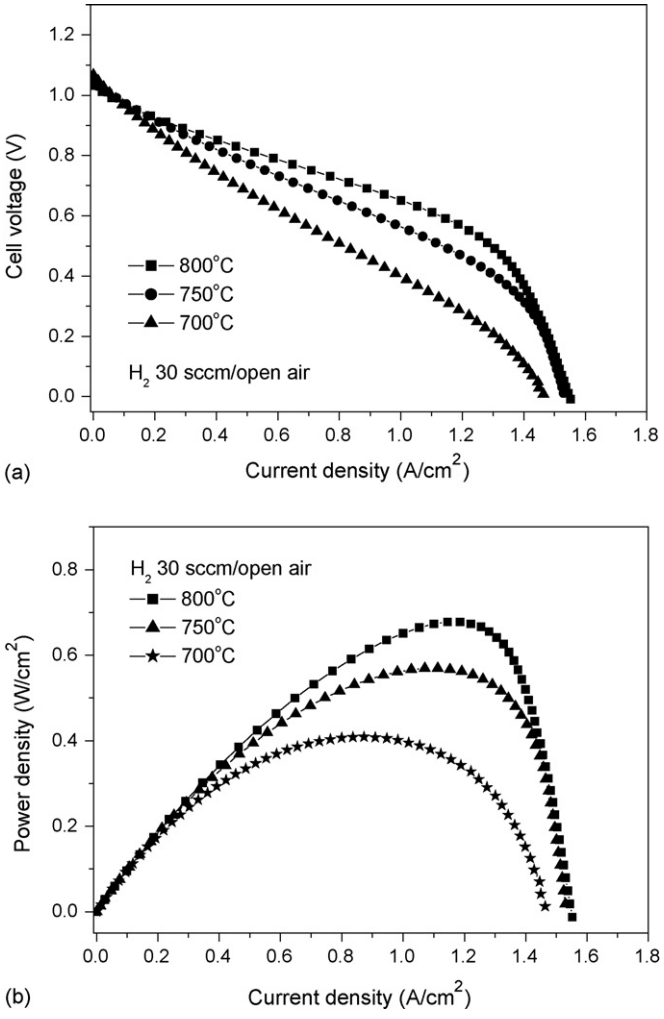

Fig. 3. (a) Cell voltage and (b) power density as function of current density of a YSZ (3 μm)/GDC (7 μm) bilayer electrolyte cell measured between 700 and 800 °C in humidified hydrogen and open air.

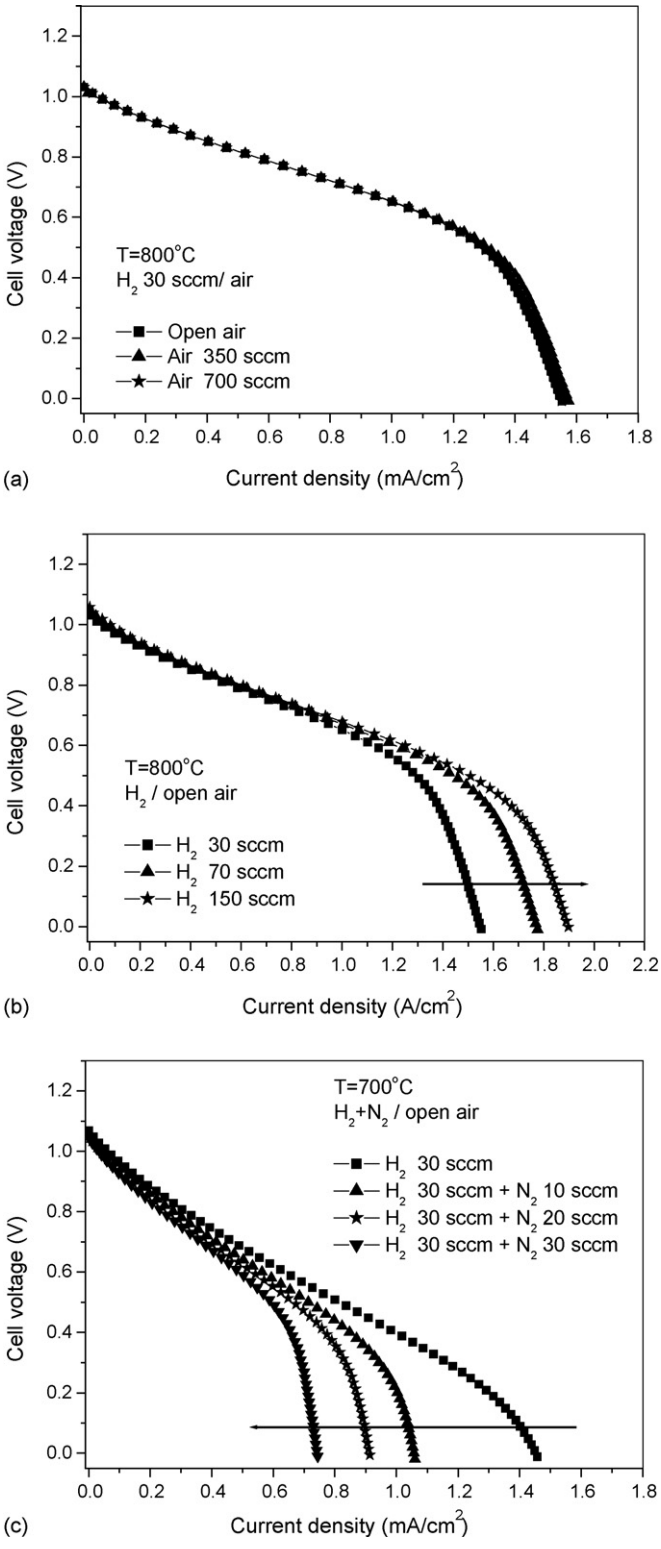

Fig. 4. Effects of (a) air and (b) hydrogen flow rates and (c) hydrogen concentration on polarization behaviour of YSZ/GDC bilayer electrolyte cell.

ness of the electrolyte films could be clearly determined under SEM. The relative density of the anode substrate before and after reduction was evaluated by the Archimedes method using water as the medium.

3. Results and discussion

3.1. Microstructure of electrolyte films

To serve effectively as an electronic blocking layer, the YSZ film is required to be dense and crack-free to avoid exposure of the GDC layer to the fuel. At the same time, the YSZ film should be deposited as thinly as possible to minimize the electrolyte resistance. Therefore, before the YSZ/GDC bilayer electrolyte film was prepared, attempts were made to deposit a thin monolayer YSZ film on the anode substrate by spray coating. After a number of trials, YSZ films with good quality and a thickness of 3 μm were deposited successfully on the anode substrate after co-sintering at 1400 °C for 2 h. Fig. 1(a) and (b) shows the surface and cross-sectional SEM images of a YSZ film on a Ni–YSZ cermet substrate (the anode substrate has been reduced to show the electrolyte film more clearly). It is seen that the YSZ film is fully dense and there are no cracks or pin-holes. The YSZ film is uniform, about 3-μm thick, and appears to be well bonded to the porous anode substrate. On this basis, deposition of YSZ/GDC bilayer electrolyte films was carried out using the same wet ceramic process and co-sintering parameters. Fig. 1(c) and (d) shows surface and cross-sectional micrographs of a YSZ/GDC bilayer electrolyte film on the reduced Ni–YSZ anode substrate. The total thickness of the bilayer electrolyte film is about 10 μm, i.e., a 3-μm YSZ layer and a 7-μm GDC layer. Despite the presence of the GDC layer on the top, the YSZ layer appears to be fully dense and to adhere to the anode substrate after co-sintering, as in the case of the monolayer YSZ film. The GDC layer is also highly dense and only a few isolated pores can be observed in the cross-section. Except for some micro-pores at the interface, an excellent bonding has been formed between the two electrolyte layers by the co-sintering process. After electrochemical testing in the fuel cell mode, no cracks are observed in the YSZ/GDC bilayer film. This indicates that the two electrolyte layers and the anode substrate thermo-mechanically match well, although some references have reported a non-negligible difference in thermal expansion coefficient (TEC) between YSZ and doped-ceria materials [22,29,30]. The good match observed here was due to interfacial diffusion during the high-temperature co-sintering that causes the formation of solid solutions at the interface of YSZ and GDC layers. Zhou et al. [30] investigated the thermal expansion behaviour of $(GDC)_x(YSZ)_{1-x}$ solid solutions in detail and found that the TEC of the $(GDC)_x(YSZ)_{1-x}$ system increases with increasing GDC fraction from that of pure YSZ ($\sim 10.7 \times 10^{-6}\,K^{-1}$) to that of pure GDC ($\sim 13.2 \times 10^{-6}\,K^{-1}$). This implies that the formation of solid solutions due to diffusion at the YSZ/GDC interface will create a functionally graded layer between the YSZ and GDC layers in terms of thermal expansion behaviour, which would help to reduce the thermo-mechanical breakdown of a fuel cell with a YSZ/GDC bilayer electrolyte.

3.2. Open-circuit voltages of cells

With quality YSZ/GDC bilayer electrolyte films, single cells were assembled using a LSCF-GDC (50:50 by weight) composite material as the cathode, and then electrochemically tested in humidified hydrogen (3 vol.% H_2O)/air atmospheres. Fig. 2 shows the open-circuit voltages (OCVs) of a YSZ/GDC bilayer electrolyte cell measured in the temperature range of 500 to 800 °C. For the purpose of comparison, theoretical and measured OCVs for a GDC and a YSZ monolayer electrolyte cell are also included in Fig. 2. The theoretical OCV values were calculated based on the Nernst equation. Compared with the GDC monolayer electrolyte cell, as can be seen from Fig. 2, the YSZ/GDC bilayer electrolyte cell displays significantly increased OCVs, which are almost the same as those of the pure YSZ electrolyte cell. For example, an OCV of 1.05 V is recorded at 800 °C for the YSZ/GDC bilayer electrolyte cell, while for the GDC monolayer electrolyte cell with the same electrolyte thickness, the OCV is only 0.59 V at the same temperature. This indicates that a YSZ thin film of 3 μm prepared by the wet ceramic co-sintering process has successfully prevented the GDC electrolyte from exposure to the gaseous hydrogen and thus protects the GDC layer from reduction. Also, OCV enhancement becomes larger at higher temperatures. This is due to the increased reducibility or electronic transference number of ceria electrolytes with increase in temperature under reducing conditions [14]. The measured OCVs of the YSZ/GDC bilayer electrolyte cell and the pure YSZ electrolyte cell are very close to the corresponding theoretical values. The slight difference observed may be due to instrumental errors such as inaccurate control of the temperature of the test station furnace or the water bubbler for hydrogen humidification.

The OCV data of fuel cells based on YSZ/doped ceria bilayer electrolyte measured in this study and reported in the literature are summarized in Table 1. Almost all the bilayer electrolytes reported in the literature have a relatively thick doped-ceria substrate (0.4–2 mm). Also, in terms of the OCV, only the bilayer electrolytes fabricated by RF ion-plating and DC sputtering are satisfactory in suppressing electronic conduction in doped-ceria electrolyte. It should be highlighted that anode-supported, thin film, bilayer electrolytes with a YSZ film as an electronic blocking layer are successfully prepared, to our knowledge, for the first time in this study using a simple and cost-effective wet ceramic co-sintering process.

3.3. Cell performance and polarization analysis

The current–voltage and current–power density characteristics of the YSZ/GDC bilayer electrolyte cell measured between 700 and 800 °C are shown in Fig. 3. The maximum power densities are 409, 570 and 678 mW cm^{-2} at 700, 750 and 800 °C, respectively. These power outputs are much lower than those for thin-film YSZ electrolyte cells reported in the literature [1,31]. It is noticeable that the current versus voltage curves exhibit a much steeper drop in the cell voltage at high current densities. This is a typical diffusion polarization behaviour, which suggests that the cell undergoes severe mass-transport limitations at high current densities. Generally, the maximum power density is reached at cell voltage of around 0.45 V. In this study, however, the cell voltage starts to deviate from the medium linear portion of the current–voltage curve and then drops drastically

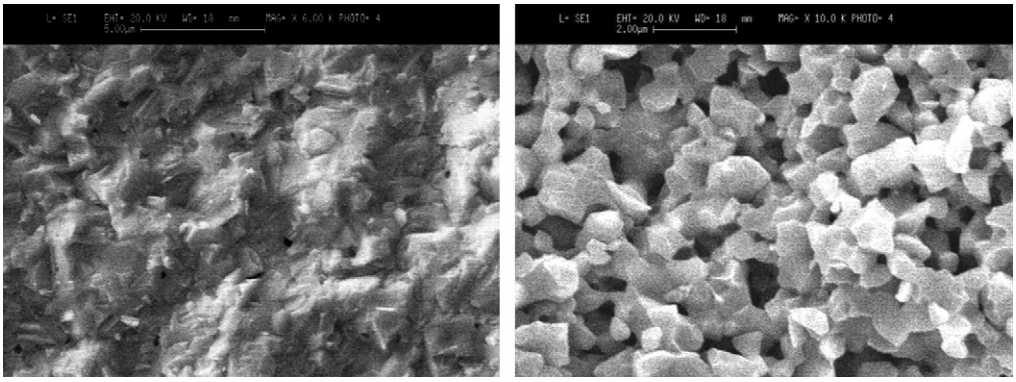

Fig. 5. Scanning electron micrographs of anode substrate sintered at 1400 °C before (left) and after (right) reduction in hydrogen.

with increasing current density from about 0.6 V at 800 °C and 0.5 V at 750 °C. This implies that the maximum power density at 800 °C is remarkably restricted by mass-transport limitation, whereas it is not affected so much at lower temperatures.

Mass-transport limitations can be caused by surface diffusion, gas diffusion, or dissociative adsorption steps. It should be noted, however, that the limiting current density does not appear to increase with increasing temperature, as shown in Fig. 3(a). This indicates that the mass-transport limitation in the present study is due to gas-diffusion limitation in the porous electrodes of the cell since the other two mechanisms are temperature-activated processes that should be strongly dependent upon the temperature [32]. The limiting current density incurred by gas diffusion limitations would increase with increasing porosity and pore size in the electrodes.

To obtain power output from a fuel cell, two gaseous reactants are generally supplied. In this study, humidified hydrogen is used as the fuel and air as the oxidant. To verify if the gas diffusion limitation is caused by hydrogen or air, the effects of air and hydrogen flow rates on the polarization behaviour of the cell have been examined at 800 °C. The results are shown in Fig. 4(a) and (b). It can be clearly seen that the limiting current density increases with increase of the hydrogen flow rate and does not change with increase of the air flow rate. This suggests that the observed diffusion polarization is due to hydrogen transport limitations at the anode. The fact that the limiting current density decreases with decreasing hydrogen concentration in the fuel gas, as shown in Fig. 4(c), further confirms that hydrogen transport limitation in the anode substrate is the reason for the limiting current behaviour shown in Fig. 3(a). The microstructure of the anode substrate before and after reduction in hydrogen is shown in Fig. 5. Before reduction, the anode substrate is almost fully dense with a relative density of 98.9%. After reduction, it displays a porosity of 17.4%. This low porosity and the relatively large thickness (∼0.8 mm) of the anode substrate well explain the hydrogen transport limitation and the resulting diffusion polarization.

To overcome the diffusion polarization caused by limited hydrogen supply, a reduction of the anode substrate thickness and/or the use of pore-formers to increase the porosity in the anode substrate can be adopted. Performance improvement with an increased anode substrate porosity will be presented in a future paper.

4. Conclusions

Thin films of YSZ (3 μm)/GDC (7 μm) bilayer electrolyte have been fabricated successfully on an anode substrate using a simple and cost-effective wet ceramic co-sintering process. Anode-supported single cells based on the bilayer electrolyte film have OCVs that are very close to the theoretical values. This implies that electronic conduction in the GDC electrolyte is effectively blocked by the YSZ film.

An anode-supported bilayer electrolyte cell exhibits severe diffusion polarization due to limited mass transport in the thick and low-porosity anode substrate, which accounts for the measured relatively low peak power densities, i.e. 409, 570 and 678 mW cm^{-2} at 700, 750 and 800 °C, respectively. To reduce diffusion polarization in the anode, a reduction of the anode substrate thickness and/or an increase in the anode substrate porosity can be considered.

References

[1] S.D. Souza, S.J. Visco, L.C.D. Joughe, Solid State Ionics 98 (1997) 57.
[2] T. Tsai, S.A. Barnett, Solid State Ionics 98 (1997) 191.
[3] T. Hibino, A. Hashimoto, K. Asano, M. Yano, M. Suzuki, M. Sano, Electrochem. Solid-State Lett. 5 (2002) A242.
[4] J.W. Yan, Z.G. Lu, Y. Jiang, Y.L. Dong, C.Y. Yu, W.Z. Li, J. Electrochem. Soc. 149 (2002) A1132.
[5] T.L. Nguyen, K. Kobayashi, T. Honda, Y. Iimura, K. Kato, A. Neghisi, K. Nozaki, F. Tappero, K. Sasaki, H. Shirahama, K. Ota, M. Dokiya, T. Kato, Solid State Ionics 174 (2004) 163.
[6] Z.P. Shao, S.M. Haile, Nature (London) 431 (2004) 170.
[7] B.C.H. Steele, Solid State Ionics 129 (2000) 95.
[8] R. Doshi, V.L. Richards, J.D. Carter, X. Wang, M. Krumpelt, J. Electrochem. Soc. 146 (1999) 1273.
[9] C.R. Xia, F.L. Chen, M.L. Liu, Electrochem. Solid-State Lett. 4 (2001) A52.
[10] R.R. Peng, C.R. Xia, X.Q. Liu, D.K. Peng, G.Y. Meng, Solid State Ionics 152/153 (2002) 561.
[11] C.R. Xia, M.L. Liu, J. Am. Ceram. Soc. 84 (2001) 1903.
[12] K. Zheng, B.C.H. Steele, M. Sahibzada, I.S. Metcalfe, Solid State Ionics 86-88 (1996) 1241.

[13] Y.J. Leng, S.H. Chan, S.P. Jiang, K.A. Khor, Solid State Ionics 170 (2004) 9.
[14] M. Mogensen, N.M. Sammes, G.A. Tompsett, Solid State Ionics 129 (2000) 63.
[15] A. Atkinson, Solid State Ionics 95 (1997) 249.
[16] S.P.S. Badwal, F.T. Ciacchi, J. Drennan, Solid State Ionics 121 (1999) 253.
[17] A.V. Virkar, J. Electrochem. Soc. 138 (1991) 1481.
[18] S.H. Chan, X.J. Chen, K.A. Khor, Solid State Ionics 158 (2003) 29.
[19] F.M.B. Marques, L.M. Navarro, Solid State Ionics 100 (1997) 29.
[20] H. Yahiro, Y. Baba, K. Eguchi, H. Arai, J. Electrochem. Soc. 135 (1988) 2077.
[21] K. Mehta, S.J. Hong, J.F. Jue, A.V. Virkar, in: S.C. Singhal, M. Dokiya (Eds.), Proceedings of Third International Symposium on Solid Oxide Fuel Cell, The Electrochemical Society, Pennington, NJ, USA, 1993, p. 92.
[22] T. Inoue, T. Setoguchi, K. Eguchi, H. Arai, Solid State Ionics 35 (1989) 285.
[23] K. Eguchi, T. Setoguchi, T. Inoue, H. Arai, Solid State Ionics 52 (1992) 165.
[24] K. Chour, J. Chen, R. Xu, Thin Solid Films 304 (1997) 106.
[25] T. Tsai, E. Perry, S. Barnett, J. Electrochem. Soc. 144 (1997) L130.
[26] K. Mehta, T. Xu, A.V. Virkar, J. Sol–Gel Sci. Technol. 11 (1998) 203.
[27] S.G. Kim, S.P. Yoon, S.W. Nam, S.H. Hyun, S.A. Hong, J. Power Sources 110 (2002) 222.
[28] W.S. Jang, S.H. Hyun, S.G. Kim, J. Mater. Sci. 37 (2002) 2535.
[29] V.V. Kharton, F.M.B. Marques, A. Atkinson, Solid State Ionics 174 (2004) 135.
[30] X.D. Zhou, B. Scarfino, H.U. Anderson, Solid State Ionics 175 (2004) 19.
[31] Y. Jiang, A.V. Virkar, J. Electrochem. Soc. 150 (2003) A942.
[32] J. Mizusaki, K. Amano, S. Yamauchi, K. Fueki, Solid State Ionics 22 (1987) 313.